

DIGITAL ADJUSTMENT OF ANALOG-TO-DIGITAL CONVERTER TRANSFER FUNCTION

Janusz Janiczek

Wrocław University of Technology, Department of Electronics, Chair of Electronic and Photonic Metrology, B. Prusa 53/55, 51-317 Wrocław, Poland (✉ janusz.janiczek@pwr.wroc.pl, +48 71 320 6290)

Abstract

The paper presents a method for digital adjustment of the analog-to-digital converter transfer function. A converter with such adjustments is a useful tool for correcting non-linearity of transducers, especially those with high linearity, in case of which the numerical correction would lead to loss of resolution.

An implementation of such a converter to adjust a carbon monoxide sensor transducer has been presented.

Keywords: correction of transducer transfer function, A/D converter.

© 2009 Polish Academy of Sciences. All rights reserved

1. Introduction

In the area of state-of-art meters and measurement systems it is clear that three-dimensionally dispersed measuring systems [5], in which a transducer and transmitting systems are placed “in-situ” in the measured object and the to-be-processed signal is transmitted to a centre, are more and more widely applied.

The connection between test points and the centre could be wired, although it usually results in a complex and extensive wiring system which can introduce additional noise, affect the reliability and increase the overall cost. Therefore nowadays wireless connections are preferred.

Wireless technology may facilitate the development of the three-dimensionally dispersed measuring system and decrease its cost. Wireless connections allow to avoid interferences caused by potential differences between particular points of the system. But the most important advantage of a wireless system over a wired one is that the transducer can be placed in a hard-to-reach place. The concrete tension measuring system where the tension transducer is imbedded in concrete along with the transmitter and feeding battery is a good example of that. Nowadays remote-read gas meters, due to novel transducers and transmitters capable to work failure-free for up to 10 years, provide another example of the usefulness of wireless systems.

A new domain of application of wireless technology are so-called intelligent transducers *i.e.* measuring transducers integrated with analog-to-digital converters and micro-controllers. Such architecture enables the development of miniaturized measurement modules with processing capability allowing to pre-process the data *e.g.* to linearize the transfer function and normalize the output signal. This is especially practicable with transducers based on silicone technology [1].

The key element of such a measuring set is an analog-to-digital converter. The ADC units implemented in micro-controllers have resolutions of 10-12 bits in case of successive approximation analog-to-digital converters or 16 bits in sigma-delta analog-to-digital converters. However because of the conversion errors metrologically they can be considered

to be 8-10-bitted. Therefore, there is a necessity to develop a simple analog-to-digital converter with low-level input current and appropriate metrological parameters.

Resistance and non-linear transducers are a very large group which should be taken into account when an analog-to-digital converter is designed. Especially, when the transducer transfer function is highly nonlinear, correction in the analog-to-digital converter is preferred [6,7, 8, 9].

2. The Method

Analysis of operation of different analog-to-digital converter modes showed that a converter with a pulse feedback [2, 3, 4] is the most suitable for this purpose. It belongs to the family of integrating converters. An advantage of the pulse system is the simplicity of its current mode logic, a disadvantage, that it converts only unipolar signals, although this limitation does not interfere with interfacing measuring transducers, especially resistive ones. Additionally their transfer functions can be processed, what considerably facilitates the correction of transducer transfer functions. The block diagram of a converter with pulse feedback is presented in Fig. 1 and the voltage transient in the converter is shown in Fig. 2.

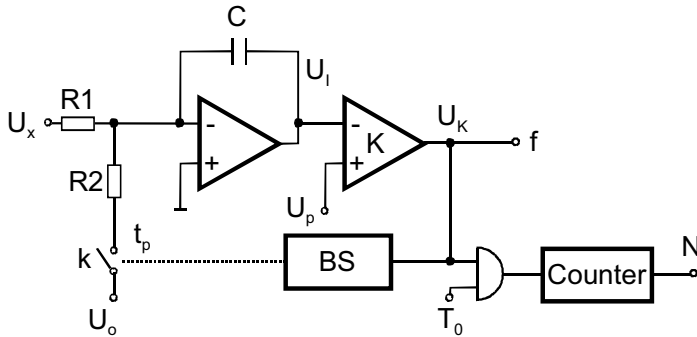


Fig. 1. Block diagram of pulse feedback converter.

The current block of this converter consists of an integrator assembled with an operating amplifier, a capacitor C, resistors R1 and R2, a comparator K, a control block BS, a switch k and a reference voltage unit U_o . The output of the comparator is a signal, the frequency f of which is a function of the input voltage U_x . If the processed output is supposed to be digital, the output signal pulses are totting up in the counter, for a T_o period of time.

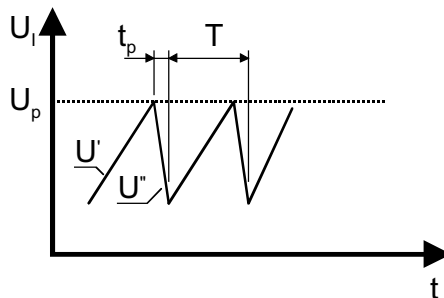


Fig. 2. Voltage transient in the converter.

The logic of this converter is that the voltage U_x is continually applied, via resistor R1, to the integrator. It causes the voltage U_I at the output of the integrator to increase until it reaches the level of reference voltage U_p . In the effect this switches on the comparator K and the control block BS. Block BS closes the switch applying a reference voltage to the integrator input, via the R2 resistor polarized opposite to the input voltage. The effect is that the voltage at the integrator output changes. After time t_p the switch is switched off and the cycle repeats.

The first stage of converter operation is described by the following formula:

$$U'(t) = \frac{1}{R_1 C} \int_0^{T-t_p} U_x(t) dt. \tag{1}$$

At the second stage, when the reference voltage is applied to the integrator, the voltage transient at the integrator output can be expressed by:

$$U''(t) = \frac{1}{R_1 C} \int_{T-t_p}^T U_x(t) dt - \frac{1}{R_2 C} \int_{T-t_p}^T U_o(t) dt. \tag{2}$$

In steady state the voltage increments at the integrator output equal:

$$U' + U'' = 0. \tag{3}$$

Hence, summarizing integrals (1) and (2) we have:

$$\frac{1}{R_1 C} \int_0^T U_x(t) dt = \frac{1}{R_2 C} \int_0^{t_p} U_o(t) dt. \tag{4}$$

Since the voltages U_x and U_o are constant, by transforming (4) we get the following expression for the frequency of the output converter signal:

$$f = \frac{1}{T} = \frac{U_x R_2}{U_o R_1 t_p} \tag{5}$$

and the number of totting-up pulses during time T_o equals:

$$N = T_o f = \frac{U_x R_2 T_o}{U_o R_1 t_p}. \tag{6}$$

The expression (4) shows that in one processing cycle, the charge applied to the integrator equals the charge led out from the integrator at the applied reference voltage U_o . The measuring time of the converted voltage U_x *i.e.* the time of totting up pulses in the counter, equals T_o and during the entire period the lead-in and lead-out charge is in equilibrium. Taking it into account, the expression (4) takes the following form:

$$\frac{1}{R_1} \int_0^{T_o} U_x(t) dt = \frac{1}{R_2} \int_0^{N t_p} U_o(t) dt. \tag{7}$$

Assuming that the reference voltage U_o changes discretely, the (7) expression can be reformulated to:

$$U_x \frac{T_0}{R_1} = \frac{N \cdot t_p}{R_2} \sum_{i=0}^{N-1} U_{oi} \tag{8}$$

If U_{oi} is constant during p sections, the expression (7) for the m -section can be expressed by:

$$U_x = \frac{R_1 t_p}{R_2 T_0} \left(p \sum_{i=0}^{m-1} U_{oi} + U_{om} (N - m \cdot p) \right) \tag{9}$$

The expression (9) shows that the transfer function of a pulse feedback converter can be adjusted by accordingly changing the reference voltage U_o during data conversion. Generating suitable U_o voltages involves the use of digital-to-analog converters, which expand the system, increases the cost and power consumption.

It can be derived from formula (9) that the converter transfer function depends on the time of feedback pulse duration t_p . In the converter shown in Fig.1 the time t_p is generated by a monostable system, what does not ensure an accuracy high enough. It can be dealt with by modifying the converter as in Fig. 3.

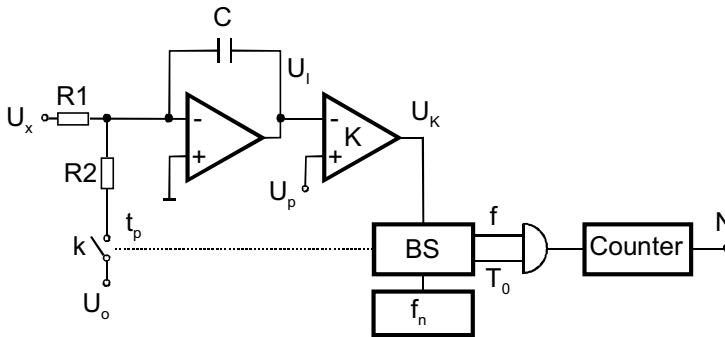


Fig. 3. Block diagram of modified pulse feedback converter.

The modified converter operates so that the start of time t_p is not at the moment of switching on the comparator but it is synchronized with the arrival of the first pulse from the generator f_n after the comparator switches on. It is illustrated in Fig. 4.

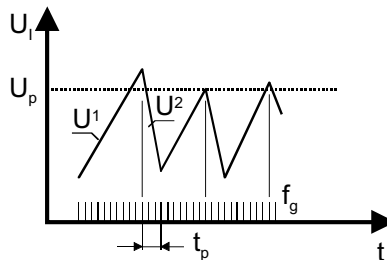


Fig. 4. Voltage transient in modified converter.

In this solution the t_p interval can be generated by dividing the f_n frequency in the divider. It causes some deviation in the output signal frequency but after averaging in the T_o period it does not effect the conversion accuracy. The same may apply to the T_o calculation. That is why T_o and t_p times can be expressed as:

$$T_0 = \frac{k}{f_n} \quad t_p = \frac{q}{f_n}. \quad (10)$$

Substituting T_0 and t_p in (9) by (10) expressions we have:

$$U_x = \frac{R_1 k}{R_2 q} \left(p \sum_{i=0}^{m-1} U_{oi} + U_{om} (N - m \cdot p) \right). \quad (11)$$

Due to this solution, the converter accuracy depends only on R_1/R_2 ratio equity and accuracy of U_o generation.

Substituting in (7) the integral by summing we have:

$$U_x \frac{T_0}{R_1} = \frac{U_o}{R_2} \sum_{i=0}^{N-1} t_{pi}. \quad (12)$$

Taking into account the (10) expressions the (12) can be expressed as:

$$U_x = \frac{R_1 U_o k}{R_2} \sum_{i=0}^{N-1} q_i, \quad (13)$$

which proves that the pulse feedback converter transfer function can be adjusted through altering of the counter divider which determines the time of pulse t_p .

Assuming as above that q_i values are constant in p periods we get:

$$U_x = \frac{R_1 U_o k}{R_2} \left(p \sum_{i=0}^{m-1} q_i + q_m (N - m \cdot p) \right). \quad (14)$$

The expression shows that in such configuration of the converter with pulse feedback it is possible to adjust, in a very wide range, the transducer transfer function approximated with a piecewise linear function. What is more, it is possible to achieve very high conversion resolution and accuracy, which depends only on the voltage stability, stability of the R_1/R_2 ratio and the reference voltage U_o constancy. The described converter can be also applied in interfacing resistance transducers, which can be put in place of the R_1 or R_2 resistors. In that case the input voltage U_x should be constant.

3. Experimental

The method described above was implemented in remote measurement of CO concentration. A TGS 203 Figaro Engineering transducer was used for this purpose. It converts the CO concentration into resistance. The transducer's range of operation is from $2 \cdot 10^{-4}\%$ to 0.8%. According to the manufacturer specifications the characteristic of the transducer is as follows:

$$R(s) = 245.66 \cdot s^{-0.95} [\Omega], \quad (15)$$

where:

- $R(s)$ – resistance of the transducer,
- s – CO concentration [%].

The transfer function of this transducer is shown in Fig. 5. It is close to a $1/x$ function. It is a highly nonlinear function.

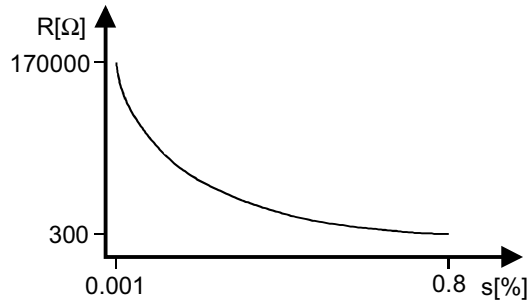


Fig. 5. The transfer function of the CO transducer.

The simplified diagram of the test setup is shown in Fig. 6.

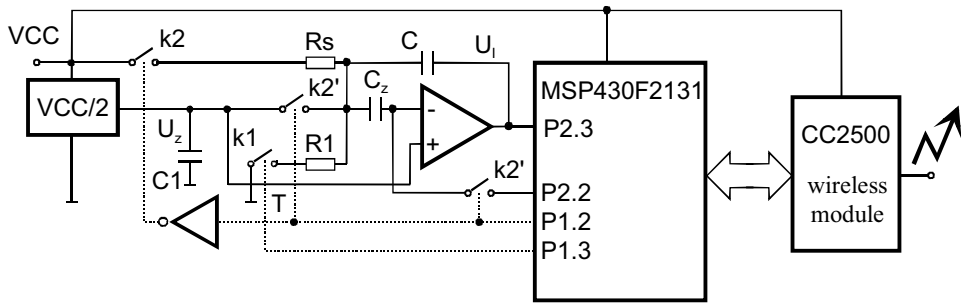


Fig. 6. Diagram of the CO measurement setup.

The ADC setup consists of an integrator equipped with an amplifier and a capacitor C , a comparator integrated into the microcontroller MSP430F2131, switches $k1$, $k2$, $k2'$, circuit dividing the voltage in half and finally a reference resistor $R1$. R_s is the resistance of the investigated transducer. Individual conversion stages are controlled by the Texas Instruments MSP430F2131 microcontroller. Additionally, in order to improve the transducer resistance to temperature and voltage surges, an additional stage in which both integrator and comparator amplifiers are reset was incorporated. The reset voltage is kept on the capacitor C_z . To avoid using two supply voltages a voltage divider was inserted into the circuit which gave the reference voltage U_z . Due to this, the voltages applied to resistors $R1$ and R_s through $k1$ and $k2$ switches have opposite polarization in reference to U_z and equal $\pm VCC/2$. The reference voltage for the comparator U_p is taken from a divider inside the microcontroller.

In the resetting stage (Fig. 7) the switches $k1$ and $k2$ are open and switch $k2'$ is closed. The integrator and comparator amplifiers are closed in a feedback loop and capacitor C_z is charged to the value of the inequality voltage of the integrator amplifier. After resetting the $k2$ switch is opened and $k2$ is closed for the entire conversion time and the converter is working in a normal pulse feedback converting mode.

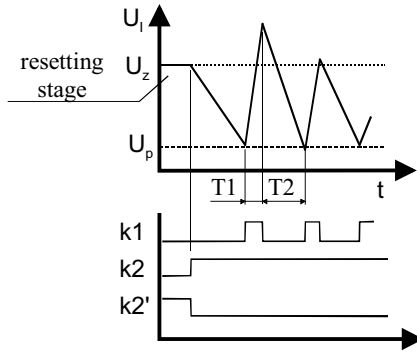


Fig. 7. Voltages at the output of the comparator.

Output pulses of the comparator are added in one of the counters integrated into the microcontroller with a second one generating T1 intervals for feedback pulses. Using the basic equation (8) describing the converter and applying formula (15) we get:

$$N = \frac{(VCC - U_z)R_1 s^{0.95}}{245.66 \cdot U_z T_2(N)} T_0, \tag{16}$$

where:

- N – impulse count from the counter,
- T_0 – conversion time.

In order to balance the load in the T_2 period it was assumed that $R_1 = 150 \Omega$, and $U_z = VCC/2$ which results in equation (16) being transformed to:

$$N = 0.61 \frac{s^{0.95}}{T_2(N)} T_0 \tag{17}$$

In order to achieve a linear relationship between the impulse count N and the CO concentration the following condition must be fulfilled:

$$T_2(N) = c \cdot s^{0.95}. \tag{18}$$

The transfer function of the transducer was approximated with ten sections which ensured that the uncertainty was less than $3 \cdot 10^{-3} \%$. Using equation (14) the variables defining T_2 were computed in Table 1.

Table 1. Values of correction coefficients .

addr.	coef.	addr.	coef.	addr.	coef.	addr.	coef.	addr.	coef.
0	256	2	77	4	43	6	23	8	10
1	112	3	57	5	32	7	16	9	4

To test the feasibility of the proposed linearization technique, the CO transducer was simulated by a resistor. Fig. 8 shows the fitting error shapes – the difference between the ideal concentration s simulated at the input and the value at the output AD converter.

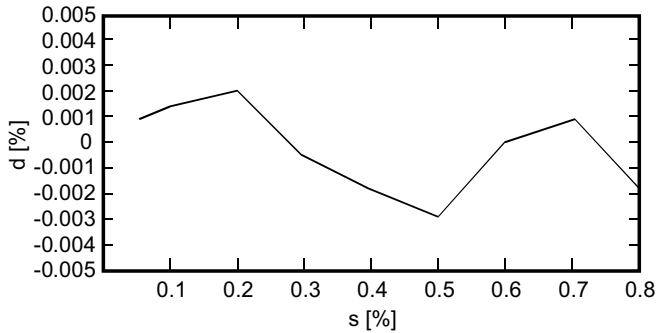


Fig. 8. The full-scale error of the analog-to-digital converter.

4. Conclusions

The conducted experiments proved the suitability of the proposed new solution of the converter. The designed analog-to-digital converter achieves a stable resolution of 14 bits. The influence of temperature in the range of 0-30 °C is less than 0.02%. The main cause of errors are variations in the resistor R1 value and changes in the VCC voltage divider. Changes in the supply voltage in the range of +/- 10 % are unnoticeable. The achieved parameters are much better than typically demanded for CO concentration measurements, however they show the capabilities of the system.

References

- [1] J. Brysek, K. Petersen, J. R. Mallon, L. Christel, F. Pourahmadi: *Silicon Sensors and Microstructures*. Nova Sensor, Silicon Valley, 1991.
- [2] J. Janiczek: "Le convertisseur analogique-numerique pour la correction des caracteristiques statiques nonlineaires des capteurs". *Measurement Science and Technology*, vol. 3, no. 4, 1992, pp. 419-420.
- [3] J. Janiczek: "Przetwornik napięcie-częstotliwość z impulsowym sprzężeniem zwrotnym". *Prace Naukowe Instytutu Metrologii Elektrycznej Politechniki Wrocławskiej. Studia i Materiały*, no. 3, 1971. (in Polish)
- [4] J. Janiczek: "Korekcja statycznych charakterystyk torów pomiarowych metodą kształtowania funkcji przetwarzania przetworników analogowo-cyfrowych". *Metrologia i Systemy Pomiarowe*, no. 5, Warszawa, 1990. (in Polish)
- [5] O. Kanoun, H.R. Tränkler: "Sensor Technology Advances and Future Trends". *IEEE Transactions on Instrumentation and Measurement*, vol. 53, no. 6, 2004.
- [6] S. Kaliyugavaradan, P. Sankaran, V. G. K. Murti: "A New Compensation Scheme for Thermistors and its Implementation for Response Linearization Over a Wide Temperature Range". *IEEE Transactions on Instrumentation and Measurement*, no. 5, 1993, pp. 952-956.
- [7] J. Mroccka: *Metrologia w procesie poznania. Współczesna metrologia – zagadnienia wybrane*. WNT, Warszawa, 2004. (in Polish)
- [8] B. Sundqvist: "Simple. wide range linear temperature-to-frequency converters using standard thermistors". *J. Phys. E. Scientific Instrum.*, vol. 16, 1983, pp. 261-164.
- [9] A.A. Khan, R. Sengupta: "A linear thermistor-based temperature-to-frequency converter using a delay network." *IEEE Transactions on Instrumentation and Measurement*, vol. IM-34, 1985, pp. 85-86.
- [10] G. Bucci, M. Faccio, C Landi. "New ADC with Piecewise Linear Characteristic: Case Study – Implementation of a Smart Humidity Sensor". *IEEE Transactions on Instrumentation and Measurement*, no. 6, 2000, pp. 1154-1166.
- [11] A. Domańska: "Elimination of Nonlinearity with Discontinuities (of the dead zone) from Static Characteristic of Converter". *Metrol Meast Syst*, vol. XV, no. 4, 2008, pp. 491-500.